Inorganic Chemistry

ARTICLE

pubs.acs.org/IC

Structural Diversity in a Series of Alkyl-Substituted Cesium Aryloxides

Timothy J. Boyle,* Leigh Anna M. Steele, Alia M. Saad, Mark A. Rodriguez, Todd M. Alam, and Sarah K. McIntyre

Advanced Materials Laboratory, Sandia National Laboratories, 1001 University Boulevard SE, Albuquerque, New Mexico 87106, United States

Supporting Information

ABSTRACT: A family of cesium aryloxides $[Cs(OAr)]_n$ were synthesized and structurally characterized from the reaction of 1:1 or 1:excess stoichiometry of Cs^0 and the appropriate alkyl-substituted phenol: 2-alkylphenol [alkyl = methyl (H-*o*MP), isopropyl (H-*o*PP), and *tert*-butyl (H-*o*BP)] and 2,6-dialkylphenol [alkyl = methyl (H-DMP), isopropyl (H-DIP), *tert*-butyl (H-DBP), and phenyl (H-DPhP)]. The products were structurally identified as $[Cs(oMP)(H\text{-}oMP)_2]_n$ (**1**), $[Cs_5(oPP)_5]_n$ (**2**), $[Cs_4(oBP)_4(H\text{-}oBP)_6]_n$ (**3x**, shown), $[Cs_3(DMP)_3]_n$ (**4**), $[Cs_2(DIP)_2]_n$ (**5**), $[Cs(DIP)(H\text{-}DIP)]_n$ (**5x**), and $[Cs(DPhP)]_n$ (**7**). Compounds **1**−**7** were found to adopt complex polymeric structures employing π interactions from the neighboring pendant phenoxide ligands. The solution behavior of these compounds was studied using solution ^{133}Cs NMR spectroscopy, and for each compound, a single ^{133}Cs NMR resonance was observed, with chemical shift values found to be strongly solvent-dependent. This implies that monomeric cesium salt species involving solvent interactions exist in solution.

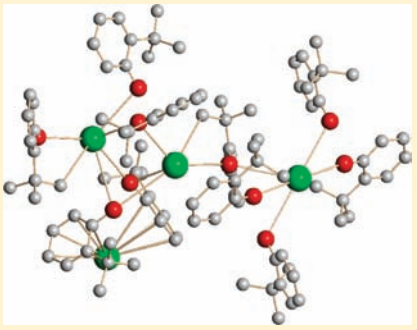

INTRODUCTION

Understanding the solid- and solution-state behavior of alkali-metal aryloxides ($[A(OAr)]_n$, where A = alkali metal) continues to be of interest. Previously, we have synthesized and reported on the structural properties of a series of $[A(OAr)]_n$, where A = Li,[1,2] K,[3] and Rb.[4] As we continue to use and explore this family of compounds in a variety of materials applications, cesium alkoxides ($[Cs(OR)]_n$) have come to the forefront for use in nitrogen−phosphorus detectors.[5,6] Understanding the structural aspects of these precursors may lend insight to optimization of the different processes discussed above; however, few crystal structures for $[Cs(OR)]_n$ are readily available.[7−14] This is surprising because these compounds have also found use in a diverse number of applications, including catalysts in organic reactions (i.e., Kolbe−Schmitt),[8] cation extraction,[9] biological fluorescent imaging,[15] and the synthesis of ceramic nanomaterials.[11]

The first structurally characterized $[Cs(OR)]_n$ was reported over 40 years ago;[16] however, in the ensuing years, only a handful of additional structures have become available.[7−14,16−23] Aryloxide (OAr) derivatives were of interest because of our previous success with the congener derivatives[1−4] as well as their ability to impart variations in the final structure; however, only the OC_6H_5 (OPh),[8] $OC_6H_3(CH(CH_3)_2)_2$-2,6 (DIP),[10] and $OC_6H_3(C_6H_5)_2$-2,6 (DPhP)[12] derivatives have been disseminated. Because of this void, we elected to synthesize and structurally characterize the "simple" *o*-alkyl-substituted phenoxide derivatives of cesium. On the basis of the expected strong interaction of the metal with neighboring phenyl rings and pendant substituents in the ortho position, elucidation of the structural aspects of $[Cs(OAr)]_n$ required single-crystal analysis.

The preferred synthesis undertaken was alcoholation of Cs^0 (eq 1), using a series of sterically varied alkyl-substituted phenols, including 2-alkylphenol [alkyl = methyl (H-*o*MP), isopropyl (H-*o*PP), and *tert*-butyl (H-*o*BP)] and 2,6-dialkylphenol [alkyl = methyl (H-DMP), isopropyl (H-DIP), *tert*-butyl (H-DBP), and phenyl (H-DPhP)] in pyridine. The products were identified as $[Cs(oMP)(H\text{-}oMP)_2]_n$ (**1**), $[Cs_5(oPP)_5]_n$ (**2**), $[Cs_4(oBP)_4(H\text{-}oBP)_6]_n$ (**3x**), $[Cs_3(DMP)_3]_n$ (**4**), $[Cs_2(DIP)_2]_n$ (**5**),[10] $[Cs(DIP)(H\text{-}DIP)]_n$ (**5x**), and $[Cs(DPhP)]_n$ (**7**).[12] The **x** in the sample number is used to indicate that an excess (xs) of HOAr was used in the preparation of the compound. The formulas reported are for the unit cell structural solutions. In order to further characterize these materials, a series of analytical investigations in both the solid and solution states were undertaken. The results of these studies are reported in detail below.

$$Cs^0 + \underset{x\,=\,1\text{ or xs}}{x\text{HOAr}} \xrightarrow{\text{py}} [Cs(OAr)]_n + H_2 \qquad (1)$$

EXPERIMENTAL SECTION

All compounds described below were handled with rigorous exclusion of air and water using standard Schlenk-line and glovebox techniques unless otherwise noted. The following reagents and solvents (Sure/Seal, 99.8+%) were used as received (Aldrich): Cs^0, H-*o*MP, H-*o*PP, H-*o*BP, H-DMP, H-DIP, H-DBP, H-DPhP, toluene (tol), and pyridine (py). Analytical data were collected on dried crystalline samples. Fourier transform infrared (FTIR) data were obtained for KBr pressed pellets

Received: July 7, 2011
Published: September 21, 2011

using a Bruker Vector 22 Instrument under an atmosphere of flowing nitrogen. Elemental analyses were performed on a Perkin-Elmer 2400 CHN-S/O elemental analyzer. Thermal gravimetric analyses (TGA) were conducted using a Mettler Toledo, TGA/DSC 1, STAR system at a ramp rate of 5 °C/min under an atmosphere of flowing nitrogen. The ^{1}H and ^{133}Cs NMR spectra were obtained on a Bruker Avance III 500 instrument, using a 5 mm BBO probe operating at 500.2 and 52.45 MHz, respectively. The ^{133}Cs chemical shifts were referenced to the external secondary standard 1 M CsCl (δ 0.0 ppm), while the ^{1}H chemical shifts were referenced to the residual pyridine solvent signal (if it could be located).

[Cs(*o*MP)(H-*o*MP)$_2$]$_n$ (1). H-*o*MP (0.080 g, 0.74 mmol) and Cs^0 (0.10 g, 0.75 mmol) were mixed in tol (~10 mL). Yield: 0.19 g (56%). FTIR (KBr pellet, cm^{-1}): 3063 (w), 3016 (w), 2923 (m, br), 2859 (w), 2562 (m, br), 2347 (w), 1899 (w), 1831 (m, br), 1587 (s), 61560 (s), 1483 (s, sh), 1466 (s, sh), 1438 (m, sh), 1280 (s), 1242 (s), 1185 (s), 1114 (s), 1041 (s), 981 (s), 930 (s), 860 (s), 757 (s), 720 (s), 596 (s), 562 (s), 530 (s), 471 (s), 445 (s). ^{1}H NMR (500.2 MHz, py-d_8): δ 7.35 (1.0H, dd, OC$_6H_5$(CH$_3$)-2), 7.25 (1.0H, dd, OC$_6H_5$(CH$_3$)-2), 7.14 (1.0H, dt, OC$_6H_5$(CH$_3$)-2), 6.81 (1.0H, dt, OC$_6H_5$(CH$_3$)-2), 2.47 (3.1H, s, OC$_6$H$_5$(CH_3)-2). ^{133}Cs NMR (52.45 MHz, py-d_8): δ 21.8. Anal. Calcd for C$_{21}$H$_{21}$CsO$_3$ (MW = 454.294): C, 55.52; H, 4.66. Found: C, 61.52; H, 5.74.

[Cs$_5$(*o*PP)$_5$]$_n$ (2). H-*o*PP (0.10 g, 0.73 mmol) and Cs^0 (0.10 g, 0.75 mmol) were mixed in tol (~10 mL). Yield: 0.16 g (89%). FTIR (KBr pellet, cm^{-1}): 3043 (s, sh), 2956 (s), 2861 (s, sh), 2659 (w), 2582 (w), 2542 (w), 2456 (w), 2419 (w), 2346 (w), 2309 (w), 2183 (w), 2151 (w), 1642 (s), 1579 (s), 1551 (s, sh), 1472 (s), 1438 (s), 1380 (s), 1343 (s), 1279 (s), 1229 (s), 1186 (s), 1152 (s, sh), 1110 (s), 1072 (s), 1031 (s), 926 (s), 891 (s), 839 (s), 767 (s), 750 (s), 587 (s), 570 (s), 538 (s, sh), 524 (s), 492 (s), 420 (s). ^{1}H NMR (500.2 MHz, py-d_8): δ 7.32 (1.0H, dd, OC$_6H_5$(CH(CH$_3$)$_2$)-2), 7.14 (1.0H, dt, OC$_6H_5$(CH(CH$_3$)$_2$)-2), 7.03 (1.0H, dd, OC$_6H_5$(CH(CH$_3$)$_2$)-2), 6.64 (1.0H, dt, OC$_6H_5$(CH-(CH$_3$)$_2$)-2), 3.78 (1.0H, sept, OC$_6$H$_5$(CH(CH$_3$)$_2$)-2, J_{H-H} = 6.9 Hz), 1.32 (6.7H, d, OC$_6$H$_5$(CH(CH_3)$_2$)-2, J_{H-H} = 7.0 Hz). ^{133}Cs NMR (52.45 MHz, py-d_8): δ 22.6. Anal. Calcd for unit cell C$_{45}$H$_{55}$Cs$_6$O$_5$ (MW = 1472.84): C, 36.66; H, 3.76. Calcd for charge balance C$_9$H$_{11}$CsO (MW = 268.09): C, 40.32; H, 4.14. Found: C, 42.69; H, 4.59.

[Cs$_4$(*o*BP)$_4$(H-*o*BP)$_6$]$_n$ (3x). H-*o*BP (0.11 g, 0.73 mmol) and Cs^0 (0.10 g, 0.75 mmol) were mixed in tol (~10 mL). Yield: 0.23 g (61%). FTIR (KBr pellet, cm^{-1}): 3052 (s), 2993 (m, sh), 2957 (s), 2911 (m, sh), 2868 (m, sh), 2699 (m, br), 2556 (m, br), 2346 (w), 1896 (m), 1587 (w, sh), 1578 (s),1556 (s), 1474 (s), 1440 (s), 1401 (m, sh), 1354 (s), 1294 (s), 1243 (s, sh), 1222 (s), 1122 (s), 1089 (s), 1049 (s), 934 (s), 858 (s), 814 (s), 767 (s), 749 (s), 683 (s), 562 (s), 500 (s), 419 (s). ^{1}H NMR (500.2 MHz, py-d_8): δ 7.48 (1.0H, dd, OC$_6H_5$-(C(CH$_3$)$_3$)-2), 7.41 (1.0H, dd, OC$_6H_5$(C(CH$_3$)$_3$)-2), 7.16 (1.0H, dt, OC$_6H_5$(C(CH$_3$)$_3$)-2), 6.76 (1.0H, dt, OC$_6H_5$(C(CH$_3$)$_3$)-2), 1.68 (8.8H, s, OC$_6$H$_5$(C(CH_3)$_3$)-2). ^{133}Cs NMR (52.45 MHz, py-d_8): δ 9.0. Anal. Calcd for C$_{50}$H$_{65}$Cs$_2$O$_5$ (MW = 1011.84): C, 59.35; H, 6.47. Found: C, 54.67; H, 6.05.

[Cs$_3$(DMP)$_3$]$_n$ (4). H-DMP (0.090 g, 0.74 mmol) and Cs^0 (0.10 g, 0.75 mmol) were mixed in tol (~10 mL). Yield: 0.17 g (89%). FTIR (KBr pellet, cm^{-1}): δ 3164 (m), 3051 (s), 2997 (s), 2960 (s), 2843 (s), 2711 (m), 2631 (w), 2588 (w), 2518 (m), 2427 (w), 2379 (w), 2306 (m), 2274 (m), 2274 (m), 2201 (w), 2157 (w), 2108 (w), 1925 (w, br), 1861 (m), 1817 (m), 1788 (m), 1640 (m), 1584 (s), 1546 (s), 1475 (s, br), 1426 (s, br), 1364 (s), 1336 (s), 1316 (s, br), 1232 (s), 1148 (m), 1086 (s), 1030 (s), 970 (s), 933 (s), 907 (s), 843 (s), 752 (s), 677 (s), 569 (s), 562 (s), 494 (s). ^{1}H NMR (500.2 MHz, py-d_8): δ 7.16 (1.9H, d, OC$_6H_3$(CH$_3$)$_2$-2,6, J_{H-H} = 7.2 Hz), 6.88 (1.0H, t, OC$_6H_3$(CH$_3$)$_2$-2,6, J_{H-H} = 7.3 Hz), 2.51 (6.3H, s, OC$_6$H$_5$(CH_3)$_2$-2,6). ^{133}Cs NMR (52.45 MHz, py-d_8): δ 15.8. Anal. Calcd for C$_{24}$H$_{27}$Cs$_3$O$_3$ (MW = 762.19): C, 37.82; H, 3.57. Found: C, 50.41; H, 5.13.

[Cs$_2$(DIP)$_2$]$_n$ (5).[10] H-DIP (0.10 g, 0.56 mmol) and Cs^0 (0.10 g, 0.75 mmol) were mixed in tol (~10 mL). Yield: 0.23 g (98%). FTIR (KBr pellet, cm^{-1}): δ 3162 (m), 3094 (m), 3057 (m), 2952 (s, br), 2863 (m, sh), 2707 (m), 2549 (m), 2483 (m), 2433 (m), 2346 (m), 2261 (m), 1891 (s), 1845 (s), 1802 (s), 1713 (s), 1582 (s), 1544 (s), 1425 (s, br), 1372 (s, sh), 1344 (s), 1283 (s), 1263 (s), 1219 (s), 1152 (s), 1131 (s), 1106 (s), 1059 (s), 1038 (s), 946 (s), 930 (s), 883 (s), 837 (s), 798 (s), 769 (s), 676 (s), 520 (s), 429 (s), 413 (s). ^{1}H NMR (500.2 MHz, py-d_8): δ 7.25 (2.1H, d, OC$_6H_3$(CH(CH$_3$)$_2$)$_2$-2,6, J_{H-H} = 7.2 Hz), 6.46 (1.0H, t, OC$_6H_3$(CH$_3$)$_2$-2,6, J_{H-H} = 7.3 Hz), 4.00 (2.1H, sept, OC$_6$H$_3$(CH-(CH$_3$)$_2$)$_2$-2,6, J_{H-H} = 6.9 Hz), 1.37 (12.2H, d, OC$_6$H$_3$(CH(CH$_3$)$_2$)$_2$-2,6, J_{H-H} = 7.0 Hz). ^{133}Cs NMR (52.45 MHz, py-d_8): δ 13.5. Anal. Calcd for C$_{24}$H$_{34}$Cs$_2$O$_2$ (MW = 620.07): C, 46.45; H, 5.53. Found: C, 47.15; H, 5.65.

[Cs(DIP)(H-DIP)]$_n$ (5x). H-DIP (1.3 g, 7.5 mmol) and Cs^0 (0.50 g, 3.8 mmol) were mixed in tol (~10 mL). Yield: 0.65 g (36%). FTIR (KBr pellet, cm^{-1}): δ 3056 (m), 2961 (s), 2865 (s), 2365 (m), 1655 (w), 1586 (s), 1459 (s, sh), 1437 (s), 1381 (s), 1359 (s), 1311 (s), 1260 (s), 1201 (s), 1171 (s), 1141 (m), 1105 (m), 1061 (w, sh), 1045 (s), 933 (s), 883 (s), 831 (s), 808 (m, sh), 752 (s), 682 (m), 582 (m), 554 (s), 537 (s), 483 (m), 426 (m). ^{1}H NMR (500.2 MHz, py-d_8): δ 7.21 (2.3H, d, OC$_6H_3$(CH(CH$_3$)$_2$)$_2$-2,6, J_{H-H} = 3.8 Hz), 6.94 (1.0H, t, OC$_6H_3$(CH$_3$)$_2$-2,6, J_{H-H} = 7.5 Hz), 3.95 (2.3H, sept, OC$_6$H$_3$(CH(CH_3)$_2$)$_2$-2,6, J_{H-H} = 6.9 Hz), 1.33 (13.2H, d, OC$_6$H$_3$(CH(CH_3)$_2$)$_2$-2,6, J_{H-H} = 7.2 Hz). ^{133}Cs NMR (52.45 MHz, py-d_8): δ 12.9. Anal. Calcd for C$_{24}$H$_{34}$CsO$_2$ (MW = 487.42): C, 59.14; H, 7.03. Found: C, 60.95; H, 7.14.

[Cs(DPhP)]$_n$ (7).[12] H-DPhP (0.19 g, 0.77 mmol) and Cs^0 (0.10 g, 0.75 mmol) were mixed in tol (~10 mL). Yield: 0.26 g (93%). FTIR (KBr pellet, cm^{-1}): δ 3080 (w, sh), 3026 (m), 3026 (m), 2950 (m, br), 1862 (m, sh), 2526 (w), 2369 (w, br), 2345 (w), 1951 (w), 1900 (w), 1872 (w), 1638 (s), 1593 (s), 1578 (s, sh), 1540 (s), 1493 (s), 1453 (s), 1413 (s), 1320 (s), 1290 (s), 1249 (s), 1183 (s), 1152 (s), 1100 (s), 1090 (s), 1073 (s), 1028 (s), 1006 (s), 991 (s), 965 (s), 951 (s), 913 (s), 854 (s), 807 (s), 760 (s), 702 (s), 619 (s), 607 (s), 597 (s), 590 (s), 573 (s), 565 (s, sh), 505 (s). ^{1}H NMR (500.2 MHz, py-d_8): δ 8.04 (4.0H, td, OC$_6H_3$(C$_6$H$_5$)$_2$-2,6), 7.47 (2.1H, d, OC$_6H_3$(C$_6$H$_5$)$_2$-2,6, J_{H-H} = 7.3 Hz), 7.32 (4.1H, tt, OC$_6H_3$(C$_6$H$_5$)$_2$-2,6), 7.14 (2.0H, tt, OC$_6$H$_3$-(C$_6H_5$)$_2$-2,6), 6.63 (1.0H, t, OC$_6H_3$(C$_6$H$_5$)$_2$-2,6, J_{H-H}= 7.3 Hz). ^{133}Cs NMR (52.45 MHz, py-d_8): δ 6.9. Anal. Calcd for C$_{18}$H$_{13}$CsO (MW = 378.2): C, 57.16; H, 3.46. Found: C, 57.36; H, 3.54.

General X-ray Crystal Structure Information. Single crystals were mounted onto a glass fiber from a pool of Fluorolube and immediately placed in a cold dinitrogen vapor stream on a Bruker AXS diffractometer employing an incident-beam graphite monochromator, Mo Kα radiation (λ = 0.7107 Å), and a SMART APEX CCD detector. Lattice determination and data collection were carried out using *SMART*, version 5.054, software. Data reduction was performed using *SAINT-PLUS*, version 6.01, software and corrected for absorption using the *SADABS* program within the *SAINT* software package. Structures were solved by direct methods, which yielded heavy atoms along with a number of the lighter atoms, or by the Patterson method, which yielded heavy atoms. Subsequent Fourier syntheses yielded the remaining light-atom positions. The H atoms were fixed in positions of ideal geometry and refined using the *APEXII* suite of software. The final refinement of each compound included anisotropic thermal parameters for all non-H atoms. Table 1 lists the unit cell parameters for the structurally characterized compounds **1**−**7**. All final CIF files were checked using the CheckCIF program (http://www.iucr.org/). Additional information concerning the data collection and final structural solutions can be found in the Supporting Information or by accessing CIF files through the Cambridge Crystallographic Data Centre database.

Specific issues with individual crystal structures follow. Compound **5** was solved in a monoclinic space group; however, both the CIF check and platon necessitated a higher-symmetry group be used. This could

Table 1. Data Collection Parameters for 1−7

	1	2	3x	4
chemical formula	$C_{21}H_{21}CsO_3$	$C_{45}H_{54}Cs_5O_5$	$C_{50}H_{65}Cs_2O_5$	$C_{24}H_{27}Cs_3O_3$
fw	454.29	1340.44	1011.84	762.19
temp (K)	173(2)	173(2)	154(2)	173(2)
space group	orthorhombic, $P2(1)2(1)2(1)$	monoclinic, $C2/c$	triclinic, $P1$	monoclinic, $C2$
a (Å)	8.6240(17)	23.547(6)	12.2711(13)	19.596(3)
b (Å)	11.687(2)	18.893(6)	12.7492(14)	10.7838(15)
c (Å)	20.052(4)	22.305(6)	17.1160(18)	12.9491(18)
α (deg)			92.199(2)	
β (deg)		92.338(6)	108.397(2)	107.988(2)
γ (deg)			106.231(2)	
V (Å^3)	2021.0(7)	9915(5)	2416.0(4)	2602.6(6)
Z	4	8	2	4
D_{calcd}(Mg/m^3)	1.493	1.796	1.391	1.945
μ(Mo Kα) (mm^{-1})	1.847	3.681	1.551	4.200
R1[a] (%; all data)	4.47 (6.30)	3.68(4.13)	3.79 (4.00)	1.66 (1.65)
wR2[b] (%; all data)	8.40 (9.01)	7.98 (8.19)	9.51 (9.69)	4.14 (4.14)

	5[10]	5x	7[12]
chemical formula	$C_{12}H_{17}CsO$	$C_{24}H_{34}CsO_2$	$C_{36}H_{26}Cs_2O_2$
fw	310.17	487.42	756.39
temp (K)	173(2)	173(2)	173(2)
space group	monoclinic, $P2/c$	triclinic, $P\bar{1}$	monoclinic, $P2(1)/c$
a (Å)	18.926(12)	10.3730(17)	11.7518(12)
b (Å)	9.408(6)	11.0123(19)	7.3162(8)
c (Å)	7.272(5)	12.413(2)	16.9431(18)
α (deg)	90	64.229(2)	
β (deg)	90.087(11)	76.297(3)	101.019(2)
γ (deg)	90	65.611(2)	
V (Å^3)	1294.9(14)	1160.1(3)	1429.9(3)
Z	4	2	2
D_{calcd} (Mg/m^3)	1.570	1.395	1.757
μ(Mo Kα) (mm^{-1})	2.829	1.611	2.581
R1[a] (%; all data)	7.64 (9.39)	5.30 (6.05)	2.38 (2.62)
wR2[b] (%; all data)	20.20 (22.35)	13.03 (13.42)	5.41 (5.54)

[a] $R1 = \Sigma||F_o| - |F_c||/\Sigma|F_o| \times 100$. [b] $wR2 = [\Sigma w(F_o^2 - F_c^2)^2/\Sigma(w|F_o|^2)^2]^{1/2} \times 100$.

not be realized because of the disorder in the pendant chains of OAr. Because this partially solved structure was found to be in agreement with the structure in ref 10, additional efforts to improve the structure of **5** were abandoned. In addition, because of the disorder in the ligand, the H atom on the aryl ring could not be identified and so was left off the structure but added to the MW and formula in the tables.

RESULTS AND DISCUSSION

The previously structurally characterized $[Cs(OR)]_n$ that do not possess a crown ether, water, or some other metal are limited, including $[Cs(OMe)]$,[23] $[Cs(OPr^i)]$,[20] $[Cs(\mu_3\text{-}OBu^t)]_4$,[7,16] $[Cs(\mu_4\text{-}OPh)]_n$,[8] $[(HOPh\text{-}Bz)_2Cs(OPh\text{-}Bz)]$ (OPh-Bz = $OC_6H_4CH_2C_6H_5$),[9] $[Cs(\mu,\eta^6\text{-}DIP)]$,[10] $[(DME)Cs(\mu_3\text{-}\eta^6\text{-}OC_6H_2(Bu^t)_3\text{-}2,4,6))]_n$ (DME = dimethoxyethane),[11] $[Cs(\mu\text{-}DPhP)]_2$,[12] $[Cs(\mu_4\text{-}OC_6H_2(NO_2)\text{-}2,4,6]$,[13,14,21] and $[Cs(BINO\text{-}H)(BINO\text{-}H_2)]$ (BINO = 1,1′-bisnaphtholate).[22] The diverse number of ligands and dearth of OAr derivatives reported[7−14] led us to investigate the changes brought through the systematic introduction of different *o*-alkyl-substituted phenolate ligands.

For the lighter congeners, the amide alcohol metathesis route proved beneficial; however, the absence of a readily available amide precursor for cesium precluded the use of this route. The majority of the $[Cs(OAr)]_n$ compounds in the literature were prepared by reacting the desired HOAr with either Cs^0 in select solvents [i.e., tetrahydrofuran (THF),[8,10] DME/tol,[11] C_6D_6[12]] or Cs(OH) in an aqueous solution.[9,13,22] Because of our success with [Rb(OAr)] from the metal and HOAr in toluene,[4] we elected to undertake the metal alcoholysis reaction pathway (eq 1) for the production of the $[Cs(OAr)]_n$ derivatives of interest.

Synthesis. Under an inert atmosphere, Cs^0 was weighed out into a vial and covered with toluene. A total of 1 equiv of the desired HOAr was slowly added, with slight bubbling noted for each reaction. Upon consumption of Cs^0, often assisted by shaking of the vial (*note!* no stir bar was used), an insoluble, off-white powder formed that could not be redissolved, even through the application of heat. However, the precipitate immediately dissolved upon the introduction of a small amount of pyridine. Interestingly, the $[Cs(DBP)]_n$ derivative (**6**) could not be solubilized

dx.doi.org/10.1021/ic201438s |*Inorg. Chem.* 2011, 50, 10363–10370

in any solvent attempted at elevated temperatures; therefore, further characterization was not undertaken for **6**. Crystals were grown by slow evaporation of the volatile component of the reaction mixture and removed for single-crystal studies. For the remainder of the bulk analyses, the mother liquor was decanted and the subsequent crystals were dried and analyzed.

FTIR Data. The dried crystalline material was first studied by FTIR spectroscopy, and no HO− stretch (∼3000 cm^{-1}) was readily identified in the spectrum for any of these compounds. This was expected for a number of the reaction products (**2**, **4**, **5**, and **7**); however, the lack of an −OH stretch for the H-OAr-solvated species **1**, **3x**, or **5x** was of interest. It is of note that each spectrum had broad baselines over this region that could easily mask the expected −OH peaks. The remainder of the spectra are unremarkable, revealing the various stretches and bends associated with the different OAr ligands employed. However, the marked differences in the spectra are surprising for such a similarly composed family of compounds. For example, the spectra of **5** and **5x** present very different stretch patterns for the aryl region despite the fact that the same aryloxide (DIP) was used for each. The structural variations based on complex inter- and intraligand interactions noted for **1**−**7** must account for the drastically different spectra obtained for these similarly ligated compounds and the "masked" −OH stretches. The assignment of Cs−O bands has not been established in the literature, and attempts to determine for these compounds were not successful because of the presence of strong out-of-plane bends for the aryl rings (∼650 cm^{-1}).

Crystal Structure. When possible, single-crystal X-ray experiments were undertaken to assist in understanding the structural properties of these compounds. The two structures isolated for DIP[10] (**5**) and DPhP[12] (**7**) were found to be in agreement with the literature reports and are not discussed in detail, but they are reported here for completeness. The complexity of the interactions of the ligands with the cesium metal centers varied through bridging (μ_x-), different ring π interactions (η^x-), and combinations (μ_x,η^x-) of these bonding modes by the pendant OAr species makes meaningful naming of these complexes difficult. All attempts have been directed toward naming of the unit cell.

For the excess-HOAr-generated compounds, a polymeric species was isolated for the *o*MP derivative. Figure 1 shows the crystal structural plot of **1x** in various stages of construction. For these structures, each Cs metal center in the unit cell (Figure 1b) possesses three *o*MP ligands. On the basis of the charge balance, two of the ligands must be considered protonated, but the protons could not be unequivocally located in the final model. As the structure is expanded based on symmetry (termed "grown"), a dinuclear species **1x** is formed (shown in Figure 1a). For **1x**, each Cs metal center possesses a single terminal and two additional *o*MP ligands that bridge to another Cs metal center; however, they do this in a different fashion. The first bridging *o*MP acts as a terminal ligand for the Cs(1A) metal center but π-binds through the phenyl ring of the *o*MP ligand to Cs(1) (termed η^6-*o*MP). The other *o*MP ligand of Cs(1a) uses its O atom to bridge to the Cs(1) metal center (μ-*o*MP) but also uses the phenyl π ring to bind back to Cs(1a) in a chelating fashion (termed μ,η^c-*o*MP). Thus, the polymeric chain is propagated through a series of μ,η^c- and η^6-*o*MP ligands. This leads to a chain of Cs−*o*MP ligands, as shown in Figure 1c. As the unit cell is further expanded, no interaction between the various chains was noted (Figure 1d).

As the steric bulk on the ligand was increased, it was expected that the complexity of the resulting $[Cs(OR)]_n$ would decrease.

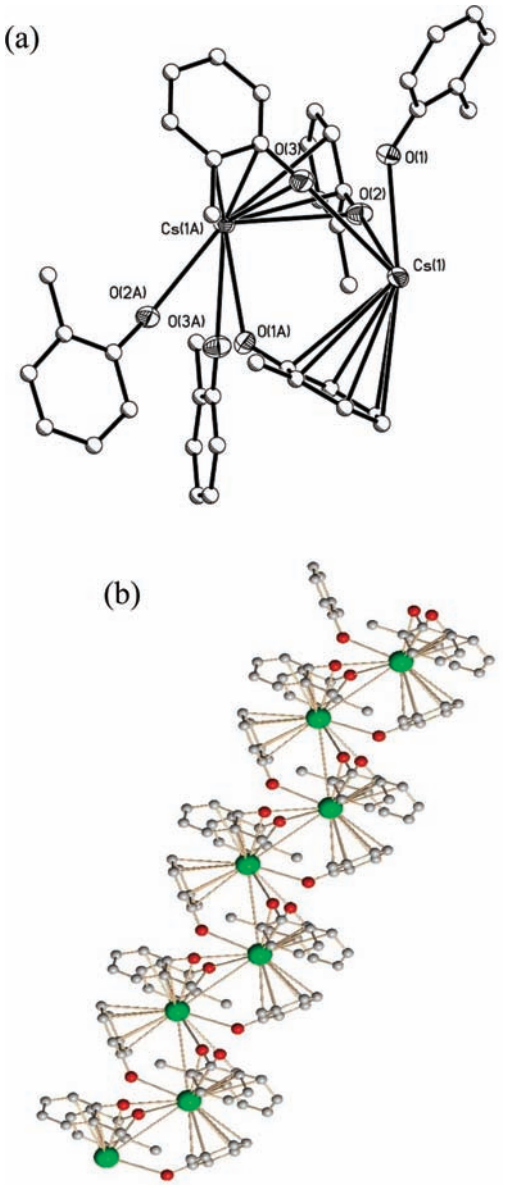

Figure 1. (a) Structural plot (grown), with thermal ellipsoids drawn at the 30% level, and (b) a packing diagram (x = 4, y = 4, and z = 1).

The use of 1 equiv of H-*o*PP led to isolation of **2**, another even more complex polymer (Figure 2) than **1**. The unit cell consists of partially formed rings with five O and six Cs atoms (Figure 2a). The atoms are arranged in a nonordered cluster in which the partial *o*PP ligands triply (μ_3-*o*PP) and doubly (μ-*o*PP) bridge to bind to the various Cs atoms. In addition, several *o*PP ligands chelate or bridge to one or more Cs metal centers using the π rings of the aryl moiety. This leads to a moiety that resembles the "$[Cs_3(\mu_3,\eta^{6c,2}$-*o*PP$)_2(\mu_3,\eta^{6c}$-*o*PP$)(\mu,\eta^3$-*o*PP$)Cs][Cs(\mu,\eta^3$-*o*PP$)Cs]$" arrangement. Upon "growing", the various ring moieties are completed and the interactions are further extended. The complex, grown structure is shown in Figure 2b, and the description of the numerous interactions is difficult to accurately state in a simple formulation. Therefore, we have opted to represent them as general bridging and π interactions (μ_x,η^x-*o*PP), where x = multiple degrees of interaction. Further expansion (Figure 2c) shows the complex interconnected final structures.

dx.doi.org/10.1021/ic201438s |*Inorg. Chem.* 2011, 50, 10363–10370

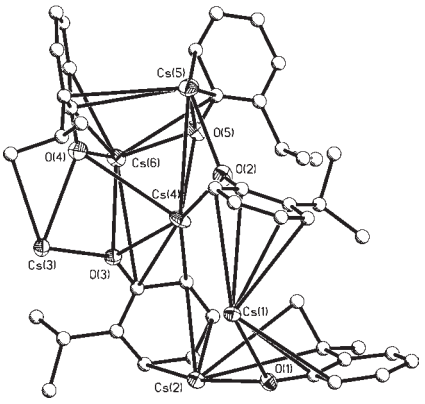

Figure 2. Structural plot of the unit cell of **2**.

The final stoichiometry appears to be the 1:1 ratio of Cs/O and is thus reported as such versus the unbalanced charge noted in the unit cell. As can be observed in Figure 2c, there is no systematic assembly of the structure of **2** and no discrete chains are available as noted for **1**.

Interestingly, the use of the *o*BP ligand does result in a significant simplification of the polymeric structure of **3x**, as seen in Figure 3. For this complex, four Cs atoms are surrounded by 10 *o*BP ligands, four of which must be considered protonated. There are three Cs atoms [Cs(1), Cs(2), and Cs(4)] that form a chain, with an additional Cs(3) off to the side of this main chain. The Cs(1) metal center has three terminal *o*BP ligands and binds to Cs(2) using one μ-*o*BP ligand. In addition, Cs(2) *o*BP ligands π-bond to Cs(1) through a π bond of one of its *o*BP ligands, while Cs(2) and Cs(4) are linked by three μ-*o*BP ligands. Two of the Cs(2) *o*BP ligands π-bond to Cs(3) in an η^6 fashion, while the other *o*BP ligand π-bonds back to Cs(2) in an η^c fashion. The final *o*BP ligand on Cs(4) is terminal and Cs(3) displays no additional bonding at this level. Obviously, the coordination environments around the Cs atoms are not complete for the [(*o*BP)Cs(η^6,μ-*o*BP)$_2$(Cs)(μ-*o*BP)Cs-(μ-*o*BP)Cs(*o*BP)$_4$] repeat moiety (Figure 3a). Because this is grown, a more complete structure is noted with long chains of "Cs(μ-*o*BP)$_3$Cs" linked by "(μ-*o*BP)Cs(*o*BP)$_4$" moieties. The η^6-bound Cs atoms link the two chains together through the π bonds, forming a 12-membered ring. Figure 3b shows the general constructs with a void space of ~17 × 13 Å. The π-bound Cs atom is not bound to any O atoms but only supported by the π ring of the *o*BP ligands. The sheet formed does not interact with any other sheets in the unit cell (Figure 3c).

The dual substitution of the ortho position of OAr typically results in a simplified structure because of the increased steric bulk. When these ligands were introduced to Cs, the structures of the resulting [Cs(OAr)]$_n$ were again complex. For **4**, the unit cell consists of three Cs atoms and three DMP ligands (Figure 4a). The central Cs(1) atom possesses two DMP ligands that η^6-bind to Cs(2) and Cs(3). The Cs(3) metal center has no additional interactions in the unit cell. Cs(1) is π-bound to the aryl ring of a DMP. This leaves a "[Cs(η^6-DMP)Cs(η^6-DMP)$_2$Cs](η^6-DMP)" moiety that employs *no* oxygen bridges available for growing (Figure 4a) the final chains. The generated chain is an intertangled mix of π-bound DMP ligands to Cs metal centers. Parts c and d of Figure 4 show the resulting complex interactions that form from these interactions.

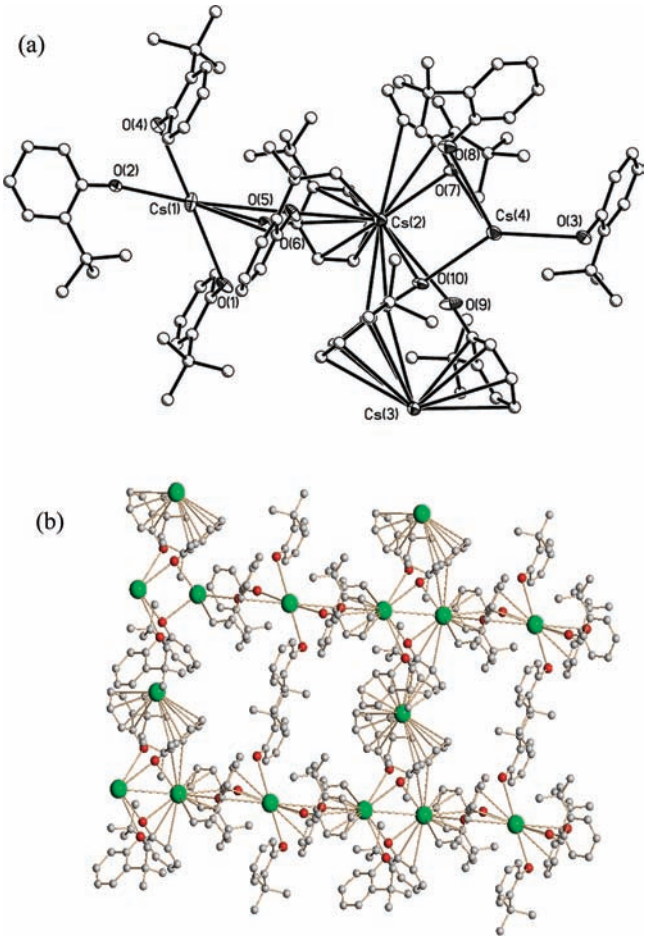

Figure 3. Structural plot of **3x**: (a) unit cell; (b) packing diagram (x = 1, y = 2, and z = 2).

It was necessary to obtain a full crystal structure of the 1:1 Cs-DIP derivative because py was used in place of THF and the unit cell parameters of **5** differed from the literature parameters.[10] While the two final structure solutions were consistent, **5** was solved in a lower space group because of ligand disorder and thus presented different unit cell dimensions. However, in the presence of excess H-DIP, a less interconnected chain was found for **5x** and is shown in Figure 5. Two DIP ligands are bound to the Cs(1) metal center, with one of the DIP ligands π-binding back to the Cs(1). The growth moiety "(η^6-DIP)Cs(DIP)" (Figure 5a) yields a complex that is interconnected through the π ring of the DIP ligands "[(η^6-DIP)Cs]$_2$(DIP)(η^6-DIP)" (Figure 5b). The full connectivity is shown by further expansion (Figure 5c) with a {[(η^6-DIP)$_2$Cs]$_2$}$_n$ repeat to form the final chain. Again, no oxygen bridges were noted for this polymer.

As mentioned, the DBP derivative was not soluble and no structure could be obtained; however, using the DPhP derivative led to high-quality crystals. The structure of **7** was found to be identical with that previously isolated.[12] A slightly improved final model isolated for **7** led to our presentation here.

In general, compounds **1**−**7** formed polymeric structures with both μ_x and η^x interactions of the pendant OAr ligands, forming chains and sheets of the various compounds. For the more sterically demanding ligands, only π bonds were used to generate the polymeric structures noted above. Even though the strong Lewis basic solvent py was used in the crystallization, no inclusion of the

dx.doi.org/10.1021/ic201438s |*Inorg. Chem.* 2011, 50, 10363–10370

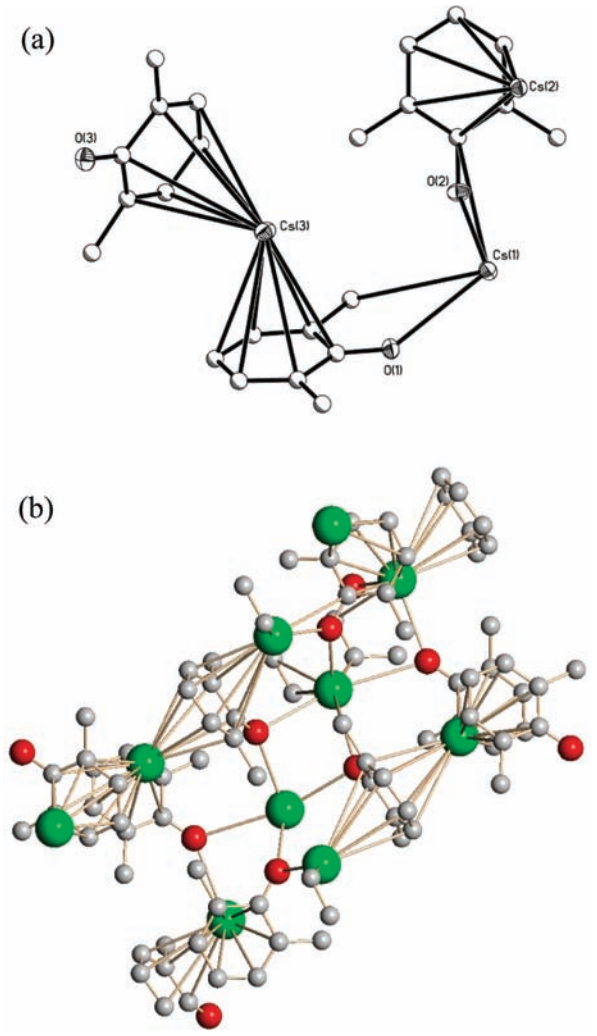

Figure 4. Structural plot of **4**: (a) unit cell; (b) structural plot (grown). Thermal ellipsoids are drawn at the 30% level.

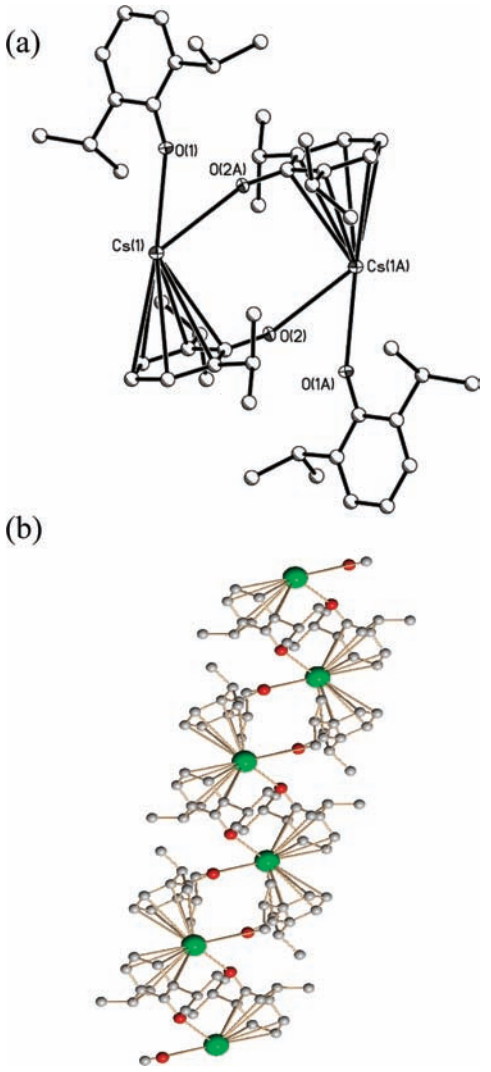

Figure 5. (a) Structural plot of **5x** (grown), with thermal ellipsoids drawn at the 30% level, and (b) a packing diagram ($x = 2$, $y = 1$, and $z = 1$).

solvent was found in any of the final structures. An investigation of their metrical data indicates that there are surprising variations noted between the different structure types isolated. Table 2 lists the metrical data obtained for **1**−**7**. The Cs−O and Cs−C_{ring} distances all fall within the literature range and are consistent with each other.[19] The Cs---Cs distances for the nearest range from 4.30 to 5.84 Å are a reflection of the different polymeric structures isolated, with the very disparate cesium arrangements present. As noted for several of these compounds, the Cs−Ph ring bonding interactions range from η^1 to η^6, within a single compound. This makes it very difficult to assign coordination numbers to the various Cs metal centers. Therefore, it is not unexpected that the angles reported for **1**−**7** are also quite varied.

Elemental Analyses. Obtaining acceptable elemental analyses for metal alkoxides typically proves difficult because of their preferential decomposition to oxides (through either thermal degradation, rapid hydrolysis, or high volatility) and, hence, their utility in the production of ceramic materials. When these characteristics are coupled with bound solvent ligands (i.e., HOAr), elemental analyses that do not agree with the single-crystal structures are common. For instance, the previously reported Cs-DIP complex had elemental analyses that were significantly varied from the calculated values;[10] however, the Cs-DPhP literature report was well within the expected CHN range.[12] Therefore, it is not surprising that all of the elemental analyses collected on the bulk powder of these compounds do not agree with the single-crystal structures, except for **7**. For the majority of the samples, a larger carbon content than expected was recorded and was attributed to residual or incorporated ligand/solvent in the bulk powder.

NMR Spectroscopy. The solution behavior of these compounds was investigated by multinuclear NMR studies. The ^{1}H NMR spectra of **1**−**7** did not contribute much information pertaining to the final solution structures, with only a single set of ligand resonances observable. Interestingly, for the aryl region of the mono-ortho-substituted derivatives [*o*MP (**1**), *o*PP (**2**), and *o*BP (**3x**)], the expected doublets and triplets were all split, while the alkyl substituent compounds displayed only one set of expected resonances. Therefore, it is presumed that the extra hydrogen splitting observed must be due to "cross-talk" between the protons on the ring or possibly from different conformers. This behavior was not observed for the disubstituted species.

Additional NMR studies were undertaken using the ^{133}Cs nuclei to give some insight into the number of unique Cs metal

Table 2. Metrical Data for 2 and 4−7

compd	Cs---Cs (Å)	Cs−O (Å)	Cs−Ph$_{cent}$ (Å)	O−Cs−O (deg)	O−Cs−Ph$_{cent}$ (deg)
1	4.95	3.42 (av)	3.75 (av)	45.42−63.42	37.80 (av)
2	4.49 (av)	2.95 (av)	3.67 (av)	72.86−95.03	32.41 (av)
3	5.84 (av)	3.31 (av)	4.07 (av)	40.20−178.39	34.48 (av)
4	4.88 (av)	3.44 (av)	3.44 (av)	73.07−110.92	44.81 (av)
5	4.98	2.84	3.49 (av)	93.19	42.16 (av)
5x	5.64	3.00 (av)	3.49 (av)	47.58	44.15 (av)
7	4.30	2.95	3.72 (av)	86.27	50.60 (av)

Table 3. ^{139}Cs Chemical Shifts for 1−7 at ∼0.10 M

sample	δ(^{133}Cs) (ppm, py-d_8)[a]	δ(^{133}Cs) (ppm, tol-d_8)[b]
1	21.8 (dil 21.3)	−82.0
2	22.6	−56.7
3x	9.0	−89.0
4	15.8	−86.2
5	13.5	—
5x	12.9	−90.0
7	6.9 (dil 7.3)	—

[a] dil = resonance observed for the diluted sample (∼0.05 M). [b] — indicates data not collected because of low solubility.

centers present for the dissolved compounds. Table 3 tabulates the resultant peaks noted for both py-d_5 and tol-d_8, and Figure 6 shows a compilation of the ^{133}Cs NMR spectra in py-d_5. Most of these compounds possessed too low a solubility in tol-d_8 to obtain a complete data set, but those collected fell within the small range of δ −80 to −90. Because of the limited number of data points, py-d_5 was used, and a significant shift to positive values ranging from δ +6.9 to +22.6 was noted for ∼0.1 M solutions of **1**−**7**. The differences in the ^{133}Cs chemical shifts between pyridine and toluene reflect the donor ability of the solvent and indicate that while pyridine is involved in the coordination environment of the Cs metal, the OAr ligands are also contributing to the chemical shift. Because pyridine solvent molecules are not observed in the single crystal isolated, oligomerization of the [Cs(OAr)]$_n$ must occur during crystallization, with the pyridine solvent molecules being forced out of the inner coordination sphere of the Cs metal.

Further, the py-d_5 ^{133}Cs chemical shifts were found to be dependent on the sample concentration, where dilution to a ∼0.05 M solution led to a +0.5 ppm chemical shift for **1** and **7**. The chemical shifts from an infinite dilution would represent a situation where only interactions between the solvent and the cesium ligand were contributing to the observed chemical shift. Therefore, this phenomenon was attributed to changes in the interaction between the cesium ligand species in solution. However, it should be noted that variation in the chemical shifts for **1** and **7** with dilution has the opposite trend in comparison to the rest of the compounds. This is assumed to be due to the interplay between the contribution of Cs−py interactions and the driving force for complexation between cesium ligand species. On the basis of these data, the crystal structures are clearly not obtained in solution, forming instead solvated salt species.

Thermal Behavior. The influence of the structural variations of **1**−**7** on the decomposition pathways was investigated by

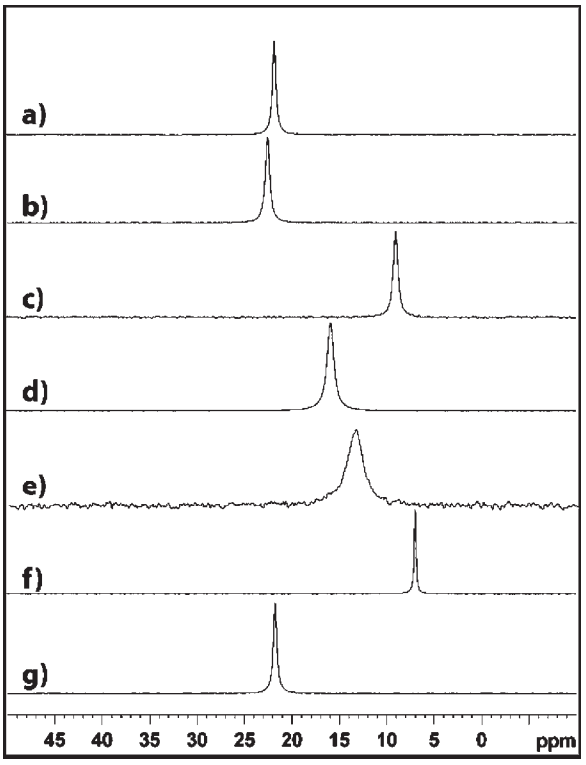

Figure 6. ^{133}Cs NMR spectra of (a) **1**, (b) **2**, (c) **3x**, (d) **4**, (e) **5**, (f) **5x**, and (g) **7**.

TGA. For each sample, weight loss occurred in several steps, except for compound **5**, which only has one weight loss step. Compounds **1** and **5x** have TGA spectrs that display no weight loss after 500 °C, with total weight losses in agreement with conversion to CsO. The remaining TGA for the other compounds have spectra that continue to show weight losses above 650 °C, and therefore it is not unexpected that the total mass changes fall short of the theoretical weight losses for each compound. While **2** did not show a distinct endotherm associated with a melt, every other sample did, with most of these occurring between 100 and 200 °C; compounds **5** and **7** displayed melt endotherms above 300 °C. The melting temperatures were redetermined using a simple melting point determination apparatus that showed the following [temp °C (compound)]: 110 (**1**), 123 (**2**), 154 (**3x**), 130 (**4**), burned (**5**), 192 (**5x**), and 320 (**7**). These were found to be in agreement. Because compounds **1**−**7** are all [Cs(OAr)]$_n$ with subtle changes in the ring substituents, the only variations noted are the structural arrangements. Therefore, any thermal variance must be attributed to the arrangement of the compounds. In particular, for **4**−**7**, the melting points should be similar because the structures vary mainly by the degree of π binding. In a review of the packing diagrams of these compounds, there is no immediate explanation of the melting behavior. The one general trend noted is that the larger the ortho substitutent on the aryloxide, the higher the melting point and decomposition temperature. Further work is necessary to uncover the connection between the thermal behavior and the structure type observed.

SUMMARY AND CONCLUSION

The first systematic study of the crystallographic nature of the family of [Cs(OAr)]$_n$ compounds was realized. For each member,

an extended polymeric structure was noted, with ligand-to-Cs π interactions playing a major role in dictating the polymerization. This is consistent with literature reports on the large affinity of Cs atoms to arene pendant moieties.[10,24,25] Increased steric bulk of the OAr substitutents did not necessarily lead to more simplistic structure types but often led to more complex inter- and intramolecular bonding that ranged from terminal to η^x-OAr to μ_x-OAr to η^x,μ_x-OAr modes. Interestingly, none of the disubstituted phenoxides displayed oxygen interconnects but relied on the π bonding of OAr. Further, while HOAr solvates have been isolated (**1**, **3x**, and **5x**), no other Lewis basic solvents (i.e., THF, py) used in the synthesis or crystallization attempts were located in the final structure. In solution, it appears that the complex bonding modes observed in the solid state have been disrupted to yield simple salts. This results in ^{133}Cs NMR resonances that are both solvent- and concentration-dependent.

■ ASSOCIATED CONTENT

Supporting Information. X-ray crystallographic data for **1**−**7** in CIF format. This material is available free of charge via the Internet at http://pubs.acs.org. These data (CCDC 830912−830918) can also be obtained, upon request, free of charge via http://www.ccdc.cam.ac.uk/conts/retrieving.html or from the Cambridge Crystallographic Data Centre, 12 Union Road, Cambridge CB2 1EZ, U.K. [fax (+44) 1223-336-033 or e-mail deposit@ccdc.cam.ac.uk).

■ AUTHOR INFORMATION

Corresponding Author

*E-mail: tjboyle@Sandia.gov. Phone: (505)272-7625. Fax: (505)272-7336.

■ ACKNOWLEDGMENT

For support of this research, the authors thank the Laboratory Directed Research and Development (LDRD) program at Sandia National Laboratories and the Office of Electricity Delivery and Energy Reliability of the U.S. Department of Energy. Sandia National Laboratories is a multiprogram laboratory managed and operated by Sandia Corporation, a wholly owned subsidiary of Lockheed Martin Corporation, for the U.S. Department of Energy's National Nuclear Security Administration under Contract DE-AC04-94AL85000.

■ REFERENCES

(1) Boyle, T. J.; Alam, T. M.; Peters, K. P.; Rodriguez, M. A. *Inorg. Chem.* **2001**, *40*, 6281.
(2) Boyle, T. J.; Pedrotty, D. M.; Alam, T. M.; Vick, S. C.; Rodriguez, M. A. *Inorg. Chem.* **2000**, *39*, 5133.
(3) Boyle, T. J.; Andrews, N. L.; Rodriguez, M. A.; Campana, C.; Yiu, T. *Inorg. Chem.* **2003**, *42*, 5357.
(4) Bunge, S. D.; Boyle, T. J.; Pratt, H. D.; Alam, T. M.; Rodriguez, M. A. *Inorg. Chem.* **2004**, *43*, 6035.
(5) Rahimian, K.; Kottenstette, R.; Stotts, L.; Martinick, K.; Wheeler, D.; Dirk, S.; Dulleck, G.; Lewis, P.; Byrnes, J. In Sandia National Laboratories Micro Chemical Analysis System for Detection of Chemical Warfare Agents (Chemical and Biological National Security Program). Spring 2009 Environmental, Monitoring and Closure Roundtable, Frisco, TX, 2009; Viewgraphs (18 pages).
(6) Kim, K.; Tsay, O. G.; Atwood, D. A.; Churchill, D. G. *Chem. Rev.* **2011**, DOI: 10/1021/cr100193y.
(7) Mann, S.; Jansen, M. *Z. Kristallogr.* **1994**, *209*, 852.
(8) Dinnebier, R. E.; Pink, M.; Sieler, J.; Stephens, P. W. *Inorg. Chem.* **1997**, *36*, 3398.
(9) Bryan, J. C.; Delmau, L. H.; Hay, B. P.; Nicholas, J. B.; Rogers, L. M.; Rogers, R. D.; Moyer, B. A. *Struct. Chem.* **1999**, *10*, 187.
(10) Clark, D. L.; Click, D. R.; Hollis, R. V.; Scott, B. L.; Watkin, J. G. *Inorg. Chem.* **1998**, *37*, 5700.
(11) Westerhausen, M.; Ossberger, M. W.; Alexander, J. S.; Ruhlandt-Senge, K. *Z. Anorg. Allg. Chem.* **2005**, *631*, 2836.
(12) Weinert, C. S.; Fanwick, P. E.; Rothwell, I. P. *Inorg. Chem.* **2003**, *42*, 6089.
(13) Harrowfield, J. M.; Skelton, B. W.; White, A. H. *Aust. J. Chem.* **1995**, *48*, 1311.
(14) Schouten, A.; Kanters, J. A.; Poonia, N. S. *Acta Crystallogr., Sect. C* **1990**, *28*, 61.
(15) Schafer, H.; Ptacek, P.; Eickmeier, H.; Haase, M. *J. Nanomater.* **2009**, Article Number 685624.
(16) Weiss, E.; Alsdorf, H.; Huhr, H. *Angew. Chem.* **1967**, *79*, 816.
(17) Allen, F. H.; Bellard, S.; Brice, M. D.; Cartwright, B. A.; Doubleday, A.; Higgs, H.; Hummelink, T.; Hummelink-Peters, B. G.; Kennard, O.; Motherwell, W. D. D.; Rodgers, J. R.; Watson, D. G. *Acta Crystallogr.* **1979**, *B35*, 2331.
(18) Allen, F. H.; Kennard, O.; Taylor, R. *Acc. Chem. Res.* **1983**, *16*, 146.
(19) Cambridge Crystallographic Data Centre, 12 Union Road, Cambridge CB2 1EZ, U.K., http://www.ccdc.cam.ac.uk; searched using *ConQuest*, version 5.31 (Nov 2009).
(20) Greiser, T.; Weiss, E. *Chem. Ber.* **1979**, *112*, 844.
(21) Herbstein, F. H.; Kapon, M.; Wielinski, S. *Acta Crystallogr., Sect B: Struct. Crystallogr. Cryst. Chem.* **1977**, *33*, 649.
(22) Grepioni, F.; Gladiali, S.; Scaccianoce, L.; Ribeiro, P.; Braga, D. *New J. Chem.* **2001**, *25*, 690.
(23) Weiss, E.; Alsdorf, H. *Z. Anorg. Allg. Chem.* **1970**, *372*, 206.
(24) Ikeda, A.; Shinkai, S. *Tetrahedron Lett.* **1992**, *33*, 7385.
(25) Ungaro, R.; Casnati, A.; Ugoozzoli, F.; Pochini, A.; Dozol, J. F.; Hill, C.; Rouquettte, H. *Angew. Chem., Int. Ed.* **1994**, *33*, 1506.